Modeling Heat and Mass Transfer in Laminar Forced Convection in A Vertical Channel: Influence of Inlet Fluid Temperature

OUEDRAOGO Rimnogdo Wilfried[1,2#] (ID), **NAMOANO David**[2], **ILBOUDO Jacques Marie**[1], **IGO Wendsida Serge**[1], **SAWADOGO Gaël Lassina**[3], **OUEDRAOGO Drissa**[3] ,

[1]Centre National de la Recherche Scientifique et Technologique/Institut de Recherche en Sciences Appliquées et Technologies/Laboratoire des Systèmes d'Énergies Renouvelables et Environnement Génie Mécanique Industriel (CNRST/IRSAT/LASERE-GMI), Ouagadougou, Burkina Faso.

[2]Laboratoire d'Energies Thermiques Renouvelables (LETRE), Université Joseph KI-ZERBO, Ouagadougou, Burkina Faso.

[3]Laboratoire de Matéraux, d'Hélio-physique et de l'Environnement (La.M.H.E),Université Nazi BONI, Bobo-Dioulasso, Burkina Faso.

How to cite this paper:
OUEDRAOGO, R.W., NAMOANO, D., ILBOUDO, J.M., IGO, W.S, SAWADOGO, G.L., OUEDRAOGO, D. (2024). Laminar Forced Convection in A Vertical Channel: Influence of Inlet Fluid Temperature. *IRA-International Journal of Applied Sciences* (ISSN 2455-4499), 19(4), 89-106. https://dx.doi.org/10.21013/jas.v19.n4.p1

IRA Academico Research is an institutional publisher member of *Publishers International Linking Association Inc. (PILA-CrossRef), USA*. IRA Academico Research is an institutional signatory to the *Budapest Open Access Initiative, Hungary* advocating the open access of scientific and scholarly knowledge. IRA Academico Research is also a registered content provider under *Open Access Initiative Protocol for Metadata Harvesting (OAI-PMH)*.

This paper is peer-reviewed under IRA Academico Research's Peer Review Program.

Rimnogdo Wilfried OUEDRAOGO (ID)/0009-0002-7324-6629

ABSTRACT

The phenomena of water vapor condensation in the presence of gas flow in channels are of considerable importance in the energy field. The aim of the present study is to investigate numerically the effect of inlet temperature on an upward laminar forced convection airflow in a channel whose walls interact with the external environment. Based on simplifying assumptions, the flow, whose thermo-physical properties depend on temperature and relative humidity, has been modeled by the Navier-Stokes equations and the flow conservation equation. The finite volume method was used to discretize the equations, and the resulting systems of algebraic equations were solved using the Thomas and Gauss algorithms. Numerical simulations carried out with fluid inlet temperatures of 305.15K, 310.15K and 323.15K and an ambient temperature of 298.15K enabled detailed study of the flow structure and hydrodynamic fields. The numerical results obtained, presented in the form of axial and radial profiles, iso values and Nusselt numbers, reveal the important role of fluid inlet temperature in heat and mass transfer in a vertical channel. The transfer rates obtained at the channel inlet and outlet are different, with latent mode heat transport dominating.

Keywords: Coupled heat and mass transfer, laminar forced convection, inlet temperature, vertical channel.

1. Introduction

Coupled heat and mass transfer has been the subject of numerous numerical and experimental studies, due to its diverse applications in fields such as fire engineering, nuclear reactors, electronic component cooling, etc. [1-7]. Parameters such as the hygrothermal properties of the fluid and the walls make channel flows complex. To find out more about the influence of these parameters on flow and transfer, Oulaid et al. [8] focused on a warm air stream with physical properties taken as constant in the first instance, and variable in the second. The authors revealed a significant discrepancy (between 8% and 30%) between the results of the two models for all hydrodynamic, thermal and mass quantities. They concluded that it was important to consider the variability of thermo-physical properties in the mathematical model. Bouchelkia et al. [9] carried out a comparative study of phase change phenomena in the flow of a thin liquid film (ethylene glycol, ethanol and water) in the presence of a laminar co-current flow of dry air in a vertical channel. The channel is made up of two parallel flat plates, the right-hand plate being subjected to a constant flow and covered by an extremely thin liquid film, while the left-hand plate is assumed to be dry and adiabatic. The variability of the thermo-physical properties of the liquid film and the gas mixture has been considered in the mathematical formulation. The results presented by the authors concern the dynamic characteristics of the fluids considered. Ethanol flow exhibits significant deceleration due to Archimedean forces, both in mass and thermal terms, while ethylene glycol flow shows little deceleration due to buoyancy forces near the interface, both in thermal and mass terms. Ethylene glycol stores more energy without changing state, due to its low specific heat and saturation pressure, while ethanol stores less energy and water can be used as a heat transfer fluid or coolant. In view of these results, the authors concluded that the evaporation phenomenon depends on the thermo-physical properties of the fluid used. Ghrissi et al. [10]

investigated the influence of air channel inlet parameters on mass and heat transfer phenomena within a water-saturated wall. Their aim was to quantify hygrothermal exchanges at the interface between a saturated porous layer and the air blown into the channel, using a mathematical model based on Darcy's model. A hybrid coupling combining both finite volume and Boltzmann methods has been proposed. Exchanges with the external environment are neglected. The authors have shown that blowing relatively moist air significantly affects heat and mass exchanges at the interface between the porous layer and the channel. On the other hand, blowing relatively dry air dries out the wall. Given the importance of parameters such as temperature, humidity and velocity, some authors have focused on their effects on heat and mass transfer. Wilfried et al [11] investigated the influence of Reynolds number on the heat and mass transfer of a fluid in laminar forced flow in a vertical channel. They demonstrated the crucial role played by the Reynolds number in enhancing heat and mass transfer. Baamrani et al. [12] studied the evaporation of a liquid film in a mixed convection flow through a vertical channel where the left wall is subjected to a uniform heat flux density and the right wall is assumed to be isolated and dry. The authors analyzed the effect of heat flux density, liquid inlet temperature and mass flow rate on heat and mass transfer. Their results show that better evaporation of the liquid film is observed for higher heat flux density and liquid inlet temperature or lower mass flow rate. Bortoli [13] numerically investigated laminar natural convection resulting from a temperature rise due to exothermic chemical reactions in square cavities. His results show that the fluid flow velocity is proportional to the heat released by the chemical reactions. An increase in fluid temperature generates a fluid movement that describes a recirculation zone located in the middle of the cavity. The energy released by the reactions in the middle of the cavity causes a temperature gradient within the cavity, giving rise to a fluid movement that descends near the walls and rises in the middle. In his thesis work, Mechergui [4] investigated the phenomenon of natural convection evaporation for laminar, two-dimensional, stationary flow in a vertical channel. The walls of the channel, on which a film of water of negligible thickness trickles, are subjected to an imposed temperature or a flow of constant density. His results showed the influence of parameters such as wall temperature, heat flux density, temperature and humidity at the channel inlet on velocity, concentration and temperature profiles inside the channel, and on heat and matter transfer. Boukadida et al. [14] analyzed coupled heat and mass transfer with forced convection evaporation in a horizontal channel. They investigated the phenomenon of water evaporation in a flow of dry air, moist air and superheated steam in an unsteady regime. By tracking the flow over time, we gain a better understanding of the coupled heat and mass transfer mechanisms at work. Their study shows that the analogy between mass and heat transfer is valid only for low temperatures and low concentrations, where heat transfer by radiation is negligible and the inversion temperature increases with the inlet flow velocity. Cherif et al. [15-16] have investigated numerically and experimentally the coupled heat and mass transfer in a vertical channel. Evaporated mass flux and thermal efficiency are calculated for different heat flux densities and flow velocities. The authors revealed that evaporation takes place over the majority of the wall surface and, in some cases, evaporative cooling occurs particularly for low heat flux and high air velocities. Kassim et al. [17] studied the effect of rising airflow humidity accompanied

by heat and mass transfer at the entrance to a vertical channel formed by two parallel flat plates, one of which is kept isothermal and humid, and the other adiabatic and dry. A thin film of negligible thickness runs down the inside face of the wet plate under gravity. The effect of Archimedes' forces on heat and mass transfer and on the hydrodynamic field was studied. The results show that these forces, opposing the upward flow, decelerate it and thus create a flow reversal near the isothermal wall. The authors also show that increasing air humidity at the channel inlet slightly reduces sensible heat transfer and increases latent heat transfer. Tsay et al. [18] analyzed the detailed heat transfer characteristics of a falling film of liquid ethanol by solving together the equations governing the liquid film and the induced flow respectively. Experimentally, they also measured the overall cooling of the film. The data measured by the authors are in good agreement with the numerical predictions. They show that cooling of the liquid film is mainly due to latent heat transfer associated with vaporization of the liquid film. The results are most significant at high inlet liquid temperatures and low liquid flow rates. Boukadida et al. [19] analyzed the effect of control parameters on air velocity, temperature and humidity inside a horizontal channel. They reveal that, as the air moves from the inlet to the outlet of the channel, its temperature, longitudinal velocity and water vapor concentration increase. Helel et al. [20] have also shown, after a numerical study of heat and mass transfer mechanisms in laminar flow, that these transfers are greater in the vicinity of the leading edge than at the outlet. Turki et al. [21] have shown that the contribution of forced convection to heat transfer is greater than that of mixed convection. The results in the literature show that the influence of inlet fluid temperature on coupled heat and mass transfer in channels has not been sufficiently investigated. This parameter plays a vital role in the condensation and evaporation phenomena that accompany fluid flows in various applications. It is obvious that an increase in fluid inlet temperature leads to an increase in flow temperature, but this temperature variation is accompanied by complex phenomena that we will investigate through numerical simulations. Our main objective is to study the influence of fluid inlet temperature on unsteady forced laminar convection flow in a vertical channel, where the thermo-physical properties of the fluid are dependent on temperature and humidity.

2. Methodology

2.1. Description of the physics model

Fluid of temperature Te, velocity Ue and relative humidity φe enters a vertical channel. The walls of the channel, of height H, are separated by a distance 2R, R being the radius of the channel. These walls undergo condensation of the water vapor contained in the fluid. Figure 1 shows the physical model of the channel under study.

2.2. Mathematical formulation

2.2.1. Simplifying hypotheses

The simplifying assumptions made in this study are :

- The flow is rotationally symmetrical around the axis (OZ);
- Transfers are two-dimensional and take place in forced laminar and unsteady regimes;

- Dufour and Soret effects are neglected;
- The radial driving pressure gradient is neglected;
- The effluent gas is laminar, incompressible and Newtonian;
- The condition of no fluid sliding on the walls is considered.

2.2.2. Transfer equations

The equations governing heat and mass transfer in the channel, based on the above assumptions, are the Navier-Stokes equations in addition to the flow conservation equation [22-23]. The thermo-physical properties of air depend on temperature and humidity. Their calculations are detailed in the work of Feddaoui et al. [24].

The radial equation of momentum

$$\rho \frac{\partial V}{\partial t} + \frac{\partial(\rho VV)}{\partial x} + \frac{\partial(\rho UV)}{\partial z} = \frac{\partial}{\partial x}\left(\mu \frac{\partial V}{\partial x}\right) + \frac{\partial}{\partial z}\left(\mu \frac{\partial V}{\partial z}\right) \tag{1}$$

The axial equation of momentum

$$\rho \frac{\partial U}{\partial t} + \frac{\partial(\rho VU)}{\partial x} + \frac{\partial(\rho UU)}{\partial z} = -\frac{\partial P}{\partial x} + \frac{\partial}{\partial x}\left(\mu \frac{\partial U}{\partial x}\right) + \frac{\partial}{\partial z}\left(\mu \frac{\partial U}{\partial z}\right) \tag{2}$$

The continuity equation

$$\frac{\partial(\rho V)}{\partial x} + \frac{\partial(\rho U)}{\partial z} = 0 \tag{3}$$

The energy conservation equation

$$\rho C_p \frac{\partial T}{\partial t} + \frac{\partial(\rho C_p VT)}{\partial x} + \frac{\partial(\rho C_p UT)}{\partial z} = \frac{\partial}{\partial x}\left(\lambda \frac{\partial T}{\partial x}\right) + \frac{\partial}{\partial z}\left(\lambda \frac{\partial T}{\partial z}\right) \tag{4}$$

The water vapor diffusion equation

$$\rho \frac{\partial C}{\partial t} + \frac{\partial(\rho VC)}{\partial x} + \frac{\partial(\rho UC)}{\partial z} = \frac{\partial}{\partial x}\left(\rho D \frac{\partial C}{\partial x}\right) + \frac{\partial}{\partial z}\left(\rho D \frac{\partial C}{\partial z}\right) \tag{5}$$

The flow rate conservation equation

$$\int_0^R U dx = Q_c + Q_e \tag{6}$$

2.2.3. Initial conditions

$$U(x,z) = 0 \; ; V(x,z) = 0 \; ; C(x,z) = C_e \; ; \; T(x,z) = T_e \tag{7a-d}$$

2.2.4. Boundary conditions

At the channel entrance: $\mathbf{z = 0; 0 \leq x \leq R}$

$$U(x,z) = \frac{3}{2}U_e\left[1 - \left(\frac{x}{R}\right)^2\right] \tag{8}$$

$$V(x,z) = 0 \; ; C(x,z) = C_e \; ; \; T(x,z) = T_e \tag{9a-c}$$

At the channel outlet:

$$\frac{\partial U(x,z)}{\partial z} = 0 \; ; \quad \frac{\partial V(x,z)}{\partial z} = 0 \; ; \quad \frac{\partial T(x,z)}{\partial z} = 0 \; ; \quad \frac{\partial C(x,z)}{\partial z} = 0 \qquad (10a\text{-}d)$$

At the axis of symmetry: $\mathbf{x = 0 ; 0 \leq z \leq H}$

$$V(x,z) = 0 \qquad (11)$$

$$\frac{\partial U(x,z)}{\partial x} = 0 \; ; \quad \frac{\partial T(x,z)}{\partial x} = 0 \; ; \quad \frac{\partial C(x,z)}{\partial x} = 0 \qquad (12a\text{-}c)$$

To the wall :

$$U(x,z) = 0 \qquad (13)$$

$$V(x,z) = V_{ev} \qquad (14)$$

Its calculation, detailed in the work of Eckert et al [25], indicates:

$$V_{ev} = -\frac{D}{(1-C_P)} \frac{\partial C}{\partial x}\bigg|_P \qquad (15)$$

The mass fraction of water vapor is given by Dalton's law:

$$C_P = \frac{P_P M_V}{[P_P M_V + (P - P_P) M_a]} \qquad (16)$$

$$-\lambda \left(\frac{\partial T}{\partial x}\right) - \rho L_V V_{ev} = -\lambda_s \left(\frac{T_{Pe} - T_{Pi}}{E}\right) = (h_R + h_C)(T_{amb} - T_{Pe}) \qquad (17)$$

The convective transfer coefficient hc is correlated with the Rayleigh number (GrPr) according to J. F Sacadura [26] :

$$h_C = \frac{Nu \lambda_{air}}{H} \qquad (18)$$

$$Nu = a(GrPr)^m \qquad (19)$$

For: $10^4 < GrPr < 10^9$; $a = 0.59$; $m = 0.25$ $\qquad (20)$

For: $10^9 < GrPr < 10^{13}$; $a = 0.21$; $m = 0.4$ $\qquad (21)$

$$Gr = \frac{g \beta_T (T_{Pe} - T_{amb}) H^3}{\vartheta_{air}^2} \qquad (22)$$

$$h_R = \gamma \sigma (T_{Pe}^2 + T_{amb}^2)(T_{Pe} + T_{amb}) \qquad (23)$$

The total heat flux exchanged between the wet wall and the flow is the sum of the sensible heat flux and the latent heat flux.

$$Q_T = Q_S + Q_L = \lambda \frac{\partial T}{\partial x}\bigg|_P + \dot{m}_C'' L_V \qquad (24)$$

$$Nu_S = \frac{Dh}{\lambda} \frac{Q_S}{(T_b - T_p)} = \frac{Dh}{(T_b - T_p)} \frac{\partial T}{\partial x}\bigg|_P \qquad (25)$$

$$Nu_L = \frac{Dh}{\lambda} \frac{Q_L}{(T_b - T_p)} = \frac{\dot{m}_C'' L_V Dh}{\lambda (T_b - T_p)} \qquad (26)$$

$$Sh = \frac{Dh}{(C_b - C_p)} \frac{\partial C}{\partial x}\bigg|_P \tag{27}$$

$$Re = \frac{UeDh}{\vartheta e} \tag{28}$$

$$Dh = 2R \tag{29}$$

$$Pr = \frac{\rho_e \vartheta_e C_{Pe}}{\lambda_e} \tag{30}$$

$$Sc = \frac{\vartheta_e}{D_e} \tag{31}$$

2.2.5. Dimensionless equations

The dimensionless equations and boundary conditions are obtained by dividing the various variables by the variables by the characteristic quantities of the system given in Table 1 (see *Figures & Tables Section*).

The radial equation of momentum

$$\rho^* \frac{\partial V^*}{\partial \tau} + \frac{\partial(\rho^* V^* V^*)}{\partial x^*} + \frac{\partial(\rho^* U^* V^*)}{\partial z^*} = \frac{\partial}{\partial x^*}\left(\frac{\mu^*}{Re}\frac{\partial V^*}{\partial x^*}\right) + \frac{\partial}{\partial z^*}\left(\frac{\mu^*}{Re}\frac{\partial V^*}{\partial z^*}\right) \tag{32}$$

The axial equation of momentum

$$\rho^* \frac{\partial U^*}{\partial \tau} + \frac{\partial(\rho^* V^* U^*)}{\partial x^*} + \frac{\partial(\rho^* U^* U^*)}{\partial z^*} = -\frac{\partial P^*}{\partial z^*} + \frac{\partial}{\partial x^*}\left(\frac{\mu^*}{Re}\frac{\partial U^*}{\partial x^*}\right) + \frac{\partial}{\partial z^*}\left(\frac{\mu^*}{Re}\frac{\partial U^*}{\partial z^*}\right) \tag{33}$$

The continuity equation

$$\frac{\partial(\rho^* V^*)}{\partial x^*} + \frac{\partial(\rho^* U^*)}{\partial z^*} = 0 \tag{34}$$

The energy conservation equation

$$\rho^* C_P^* \frac{\partial T^*}{\partial \tau} + \frac{\partial(\rho^* C_P^* V^* T^*)}{\partial x^*} + \frac{\partial(\rho^* C_P^* U^* T^*)}{\partial z^*} = \frac{1}{PrRe}\left[\frac{\partial}{\partial x^*}\left(\lambda^* \frac{\partial T^*}{\partial x^*}\right) + \frac{\partial}{\partial z^*}\left(\lambda^* \frac{\partial T^*}{\partial z^*}\right)\right] \tag{35}$$

The water vapor diffusion equation

$$\rho^* \frac{\partial C^*}{\partial \tau} + \frac{\partial(\rho^* V^* C^*)}{\partial x^*} + \frac{\partial(\rho^* U^* C^*)}{\partial z^*} = \frac{1}{ScRe}\left[\frac{\partial}{\partial x^*}\left(\rho^* D^* \frac{\partial C^*}{\partial x^*}\right) + \frac{\partial}{\partial z^*}\left(\rho^* D^* \frac{\partial C^*}{\partial z^*}\right)\right] \tag{36}$$

The flow rate conservation equation

$$\int_0^{R^*} U^* dx^* = Q_c^* + Q_e^* \tag{37}$$

2.2.6. Initial conditions

$$U^*(x^*, z^*) = 0 \; ; \; V^*(x^*, z^*) = 0 \; ; \; T^*(x^*, z^*) = 1 \; ; \; C^*(x^*, z^*) = 1 \tag{38a-d}$$

2.2.7. Boundary conditions

At the channel entrance; $z^* = 0 \; ; 0 \le x^* \le R^*$

$$U^*(x^*, z^*) = \frac{3}{2}\left[1 - \left(\frac{x^*}{R^*}\right)^2\right] \tag{39}$$

$$V^*(x^*,z^*) = 0 \; ; \; T^*(x^*,z^*) = 1 \; ; \; C^*(x^*,z^*) = 1 \tag{40a-c}$$

To the wall: $\mathbf{x^* = R^* \; ; \; 0 \leq z^* \leq H^*}$

$$U^*(x^*,z^*) = 0 \; ; \; V^*(x^*,z^*) = V_{ev}^* \tag{41}$$

$$V_{ev}^* = -\frac{D}{DhU_e\left(1/_{C_e - C_p^*}\right)} \frac{\partial C^*}{\partial x^*}\Big|_P \tag{42}$$

$$C_p^* = \frac{P_P^* - M_v^*}{P_P^* M_v^* + (P^* - P_P^*)M_a^*} \tag{43}$$

$$\lambda^*\left(\frac{\partial T^*}{\partial x^*}\right) - \frac{\rho^* L_V V_{ev} Dh}{\lambda_e T_e} = \lambda_S^*\left(\frac{T_{Pi}^* - T_{Pe}^*}{E^*}\right) = \frac{Dh}{\lambda_0}(h_R + h_C)(T_{Pe}^* - T_{amb}^*) \tag{44}$$

At the axis of symmetry: $\mathbf{x^* = 0 \; ; \; 0 \leq z^* \leq H^*}$

$$\partial V^*(x^*,z^*) = 0 \tag{45}$$

$$\frac{\partial U^*(x^*,z^*)}{\partial x^*} = 0 \; ; \; \frac{\partial T^*(x^*,z^*)}{\partial x^*} = 0 \; ; \; \frac{\partial C^*(x^*,z^*)}{\partial x^*} = 0 \tag{46a-c}$$

At the channel outlet: $\mathbf{z^* = H^* \; ; \; 0 \leq x^* \leq R^*}$

$$\frac{\partial U^*(x^*,z^*)}{\partial z^*} = 0 \; ; \; \frac{\partial V^*(x^*,z^*)}{\partial z^*} = 0 \; ; \; \frac{\partial T^*(x^*,z^*)}{\partial z^*} = 0 \; ; \; \frac{\partial C^*(x^*,z^*)}{\partial z^*} = 0 \tag{47a-d}$$

The Nusselt and Sherwood numbers become:

$$Nu_S = \frac{1}{(T_b^* - T_p^*)}\frac{\partial T^*}{\partial x^*}\Big|_p \tag{48}$$

$$Nu_L = \frac{\dot{m}_C'' L_V Dh}{\lambda_e \lambda^* T_e (T_b^* - T_p^*)} \tag{49}$$

$$Sh = \frac{1}{(C_b^* - C_p^*)}\frac{\partial C^*}{\partial x^*}\Big|_p \tag{50}$$

2.3. Numerical methodology

The discretization of equations (32), (34), (35) and (36) by the finite volume method [17] leads to an algebraic equation system of N equations with N unknowns. Each equation system obtained is tri-diagonal and is therefore solved by Thomas' algorithm. As for equation (33), it leads to a system of N equations with (N+1) unknowns. For this, it is completed by equation (37) and then solved by the Gauss algorithm. The convergence criterion chosen is:

$$\frac{\phi^{k+1}(I,J) + \phi^k(I,J)}{\phi^{k+1}(I,J)} < 10^{-5} \tag{51}$$

k represents in this expression, the number of iterations and $\mathbf{\Phi} = T^*, C^*, U^*, V^*$.

3. Results and discussions

3.1. Model validation

To validate our numerical calculation code, we compared our numerical results with those of Othmane [25], for a stationary flow with mass transfer (see Figure 2). The relative error resulting from comparison of the two results is of the order of 7%.

3.2. Mesh sensitivity study

To ensure that our results are independent of the mesh, a mesh sensitivity study was carried out. This study showed that the mesh size (41x112), even quadrupled, did not significantly modify the sensitive Nusselt (see Table 2). Consequently, the mesh (41x112) was retained for the rest of the study.

3.3. Influence of fluid inlet temperature

The results are recorded when the regime stabilizes at a time t = 3500s and are presented in tabular, profile and iso-value form under the following conditions: the fluid temperature at the channel inlet varies from 305.15 to 323.15K, with a relative humidity of 60% and a Reynolds number equal to 500. The height H considered is 1.5 m and the radius R is 0.45 m. The Figure 3 shows the thermal field of the channel flow as a function of inlet temperature.

The thermal field has iso values that increase with the temperature imposed at the inlet. This is because the temperature of the flow increases as that of the fluid at the channel inlet increases. This leads to an increase in thermal agitation and therefore in thermal gradients between the fluid and the wall. This increase in temperature influences heat and mass transfer, which will be elucidated later.

The Figure 4 shows the dynamic field of the channel as the fluid inlet temperature increases. Flow velocity increases as fluid inlet temperature rises. In fact, the increase in air flow drawn in at the inlet due to the increase in temperature and concentration gradients, combined with the decrease in viscous forces, leads to an increase in flow velocity. This increase in velocity helps improves convective transport.

The Figure 5 shows the axial evolution of mass fraction for a fluid inlet temperature equal to 323.15K and a Reynolds number equal to 500. As the fluid moves through the channel, the moisture content of the flow decreases due to changes in the state of the water vapor in the air. This water vapor condenses on the wall, making the fluid drier and drier, while releasing heat which contributes to increasing sensible heat transport in the flow.

The fFgure 6 shows the evolution of the local latent Nusselt as a function of the fluid inlet temperature. The Latent Nusselt number shows large values at the channel inlet and smaller values at the outlet. This is due to the high mass gradients in the inlet zone. At the channel outlet, these gradients become small due to wall heating and condensation. We also observe a gradual decrease in the latent Nusselt number as the fluid inlet temperature rises, thanks to condensation, which dries out the fluid more as the temperature rises.

The Figure 7 shows the evolution of the Sensible Nusselt number along the channel as a function of fluid inlet temperature. The Nusselt number shows positive values throughout the channel, reflecting heat transfer from the flow to the wall. An increase in the inlet temperature of the fluid leads

to an increase in the sensitive Nusselt number, and therefore to a rise in temperature within the channel. This is due to condensation at the wall. This phenomenon releases heat which is absorbed by the flow, contributing to the increase in sensible mode heat transport, hence the increase in the sensible Nusselt number. The profiles show high values at the channel inlet and lower values at the outlet. This is due to the steep thermal gradients at the channel entrance. At the channel outlet, these gradients become small due to wall heating and the evacuation of water vapour contained in the fluid. Heat transfer within the flow is dominated by latent mode heat transport.

The Sherwood number characterizing mass transfer between the flow and the wall is shown in Figure 8. Heat and mass exchanges between the wall and the fluid are represented by the Nusselt and Sherwood numbers. The values of the Sherwood number are positive along the entire length of the channel, reflecting the direction of mass transfer from the flow to the walls. The Sherwood number decreases with increasing fluid inlet temperature. This is because increasing fluid temperature at the channel inlet leads to a reduction in water vapor in the flow, which in turn reduces mass transfer.

4. Conclusion

In this work, we carried out a numerical study of coupled heat and mass transfer in a vertical channel whose heat exchange with the outside environment is governed by natural convection and radiation. Forced laminar flow was modeled by the Navier-Stokes equations and the flow conservation equation. These equations were discretized using the finite volume method and then solved using the Thomas and Gauss algorithms. The influence of fluid temperature at the channel inlet on heat and mass transfer was a particular focus of attention. A numerical simulation of the velocity, temperature and mass fields was therefore carried out, considering inlet temperatures of 305.15K, 310.15K and 323.15K, with an ambient temperature of 298.15K. The thermo-physical properties of the fluid are dependent on temperature and humidity. Our numerical results indicate that an increase in fluid inlet temperature leads to an increase in sensible-mode heat transfer and a decrease in latent-mode heat transfer. Material transfer between the flow and the wall shows a decrease in exchanges as the fluid inlet temperature increases. Mass and thermal gradients evolve differently as water vapor condenses, releasing heat.

Nomenclatures
A*: Dimensionless value
T: Temperature (K)
H: Channel height (m)
R: Channel radius (m)
V: Radial velocity (m.s^{-1})
U: Axial velocity (m.s^{-1})
t: Time (s)
P: Pressure (N.m^{-2})
Cp: Thermal mass capacity (JKg^{-1}.K^{-1})
Q: Flow rate (m^3.s^{-1})

D: Diffusion coefficient ($m^2.s^{-1}$)

L: Latent heat ($J.Kg^{-1}$)

E: Thickness (m)

h: Heat transfer coefficient ($W.m^{-2}.K^{-1}$)

M: Molar mass ($Kg.mol^{-1}$)

Gr: Grashof number

Re: Reynolds number

Nu: Nusselt number

Sh: Sherwood number

Pr: Prandtl number

Sc: Schmidt number

g: Accelerating gravity ($m.s^{-2}$)

β: Thermal expansion coefficient (K^{-1})

ϑ: Kinematic viscosity ($m^2.s^{-1}$)

μ: Dynamic viscosity ($Kg.m^{-1}.s^{-1}$)

σ: Stefan Boltzmann's constant ($W.m^{-2}.K^{-4}$)

Dh: Hydraulic diameter (m)

$\ddot{m}''$: Evaporated mass flow rate ($Kg.s^{-1}$)

λ: Thermal conductivity ($W.m^{-1}.K^{-1}$)

ρ: Density ($Kg.m^{-3}$)

Competing interests : Authors have declared that no competing interests exist.

Authors' contributions : This work was carried out in collaboration among all authors. All authors read and approved the final manuscript

Disclaimer (AI Usage) : Author(s) hereby declare that NO generative AI technologies such as Large Language Models (ChatGPT, COPILOT, etc) and text-to-image generators have been used during writing or editing of manuscripts.

References
[1]. M. Asbik et al. (2007). Analytical study of film-type laminar condensation of a saturated vapor in a vertical channel whose walls are covered with a porous layer. *13th international thermal days*. 1-5. Albi. French.

[2]. A. I. Alsabery et al. (2022). Impacts of two-phase nanofluid approach toward forced convection heat transfer within a 3D wavy horizontal channel. *Chinese Journal of Physics*. 77:350-365. https://doi.org/10.1016/j.cjph.2021.10.049.

[3]. M. Oubella et al. (2015). Numerical study of heat and mass transfer during evaporation of a thin liquid film. *Thermal Sciences.* 19(5):1805–1819. https://doi.org/10.2298/TSCI1301281450.

[4]. O. Mechergui. (2017). Numerical study of mass and heat transfers in natural convection in a channel: influence of the shape of the wall. University of Perpignan. French.

[5]. S. Baragh et al. (2018). An experimental investigation on forced convection heat transfer of single-phase flow in a channel with different arrangements of porous media. *Int. J. Therm. Sci.* 134:370–379. https://doi.org/10.1016/j.ijthermalsci.2018.04.030.

[6]. M. M. Ikram et al. (2020). Conjugate forced convection transient flow and heat transfer analysis in a hexagonal, partitioned, air filled cavity with dynamic modulator. *Int. J. Heat Mass Transf.* 167. https://doi.org/10.1016/j.ijheatmasstransfer.2020.120786.

[7]. V. H. Fanambinantsoa et al. (2016). Numerical study of forced convection in a horizontal rectangular channel provided with a sinusoidal protuberance. *Afrique Sciences.* 12(6) :353–364. https://www.researchgate.net/publication/331833367. French

[8]. O. Oulaid et al. (2009). Effect of the variability of thermo-physical properties on coupled heat and mass transfers in a vertical channel. *14th International Thermal Days.* Tunisia. French

[9]. I. Bouchelkia et al. (2017). Comparative numerical study of the evaporation by mixed convection of a liquid film (ethanol, water, ethylene-glycol) in a vertical channel. *XXIII French Congress of Mechanics.* Lille. French

[10]. W. Ghrissi et al. (2022). Study of the influence of input parameters in an air channel on mass and heat transfer phenomena within a wall saturated with water: application to the renovation of old wet buildings. *Journal of Building Performance Simulation.* 15(1):81–96. https://doi.org/10.1080/19401493.2021.1994651.

[11]. W. R. Ouedraogo et al. (2024). Modeling heat and mass transfer in laminar forced convection in a vertical channel: Influence of Reynolds number. *Physical Science International Journal.* 28-5):48–61. https://doi.org/10.9734/psij/2024/v28i5847.

[12]. H. E. Baamrani et al. (2021). Volume of Fluid (VOF) Modeling of Liquid Film Evaporation in Mixed Convection Flow through a Vertical Channel. *Mathematical Problems in Engineering.* https://doi.org/10.1155/2021/9934593.

[13]. A. L. De Bortoli. (2003). Mixing and chemical reacting flow simulations inside square cavities. *Applied Numerical Mathematics.* 47:295–303. https://doi.org/10.1016/S0168-9274(03)00082-5.

[14]. N. Lefi et al. (2008). Coupled transfers of heat and mass during the evaporation of liquids in an unsteady state. *Renewable Energy Review CISM'08 Oum El Bouaghi.* 217 – 225. French

[15]. A. S. Cherif et al. (2010). Intensification of the liquid film evaporation in a vertical channel. *Desalination.* 250(1):433–437. https://doi.org/10.1016/j.desal.2009.09.071.

[16]. A. S. Cherif et al. (2011). Experimental and numerical study of mixed convection heat and mass transfer in a vertical channel with film evaporation. *International Journal of Thermal Science.* 50(6):942–953. https://doi.org/10.1016/j.ijthermalsci.2011.01.002.

[17]. M. A. Kassim et al. (2010). Combined heat and mass transfer with phase change in a vertical channel. *Computational Thermal Sciences.* 2(4):299-310. https://doi.org/10.1615.

[18]. Y. L. Tsay et al. (1990). Cooling of a falling liquid film through interfacial heat and mass transfer. *International Journal of Multiphase Flow.* 16(5):853–865.

[19]. N. Boukadida et al. (2001). Mass and heat transfer during water evaporation in laminar flow inside a rectangular channel-Validity of heat and mass transfer analogy. *International Journal of Thermal Science.* 40(1): 67–81. https://doi.org/10.1016/S1290-0729(00)01181-9.

[20]. D. Helel et al. (2007). Heat and mass transfer in an unsaturated porous medium subjected to laminar forced convection. *13th international thermal days.* Albi. French.

[21]. S. Turki et al. (2003). Two-dimensional laminar fluid flow and heat transfer in a channel with a built-in heated square cylinder," *International Journal of Thermal Science.* 42():1105–1113. https://doi.org/10.1016/S1290-0729(03)00091-7.

[22]. S. Zermane et al. (2005). Numerical study of laminar mixed convection in ventilated cavities. *Science & Technology* .23 :34-44. French.

[23]. D. M. Diallo. (2010). Mathematical modeling and numerical simulation of hydrodynamics: case of flooding downstream of the Diama. University of Franche-Comté, France. French.

[24]. M. Feddaoui et al. (2003). Cocurrent turbulent mixed convection heat and mass transfer in falling film of water inside a vertical heated tube. *International Journal of Heat and Mass Transfer.* 46(18):3497–3509. https://doi.org/10.1016/S0017-9310(03)00129-7.

[25]. E. R. Eckert et al. (1972). Analysis of heat and mass transfer. New York.

[26]. J. F. Sacadura. (2015). Thermal transfers: Introduction and deepening. Paris, France. French

[27]. O. Oulaid. (2010). Coupled transfer of heat and mass by mixed convection with phase change in a channel. University of Sherbrooke. French.

FIGURES & TABLES
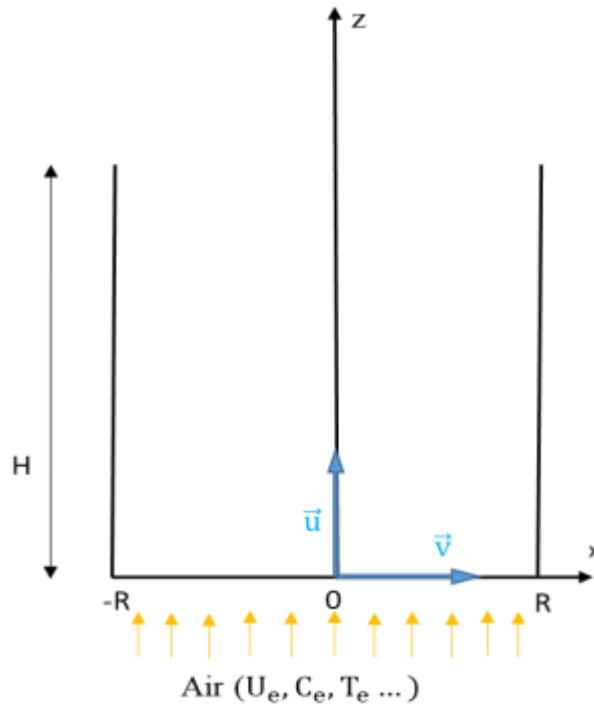
Figure 1. The physical model
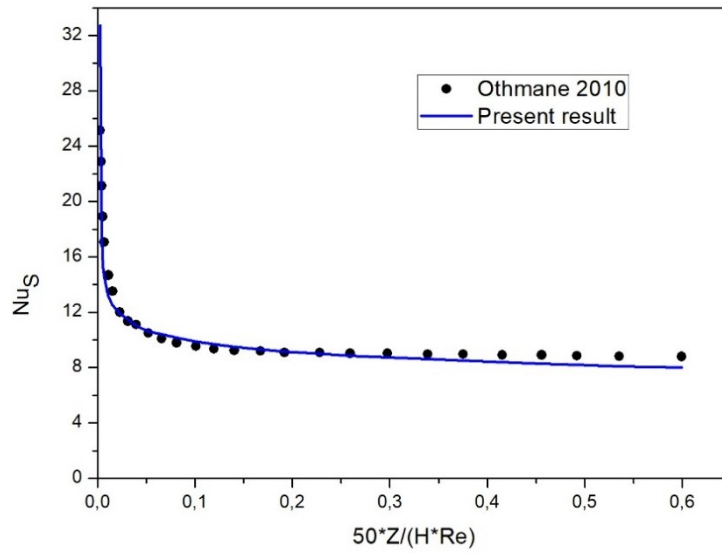
Figure 2. Validation of the numerical code (To = 20°C, Tw = 40°C, φo = 50%, Pr = 0.703, Sc = 0.592, Re = 400).
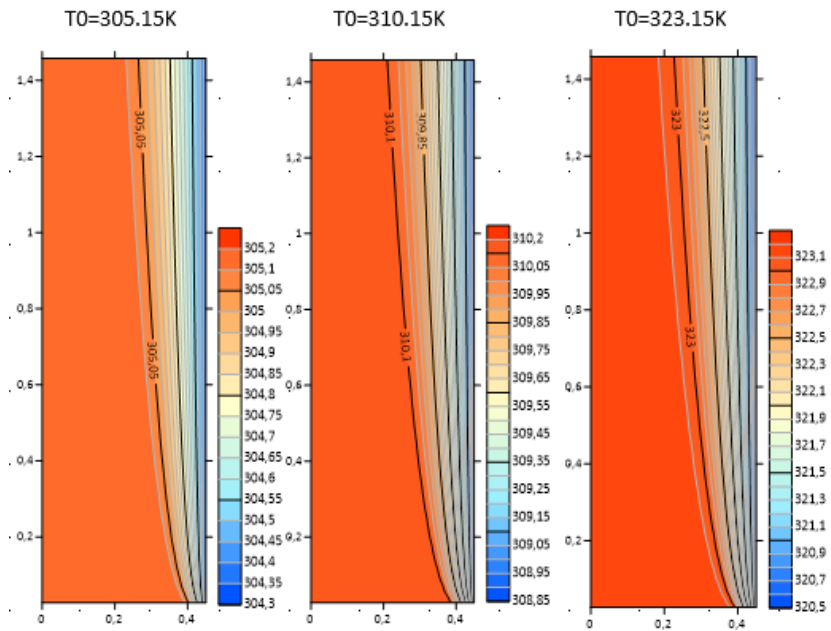
Figure 3. Thermal flow field as a function of inlet temperature
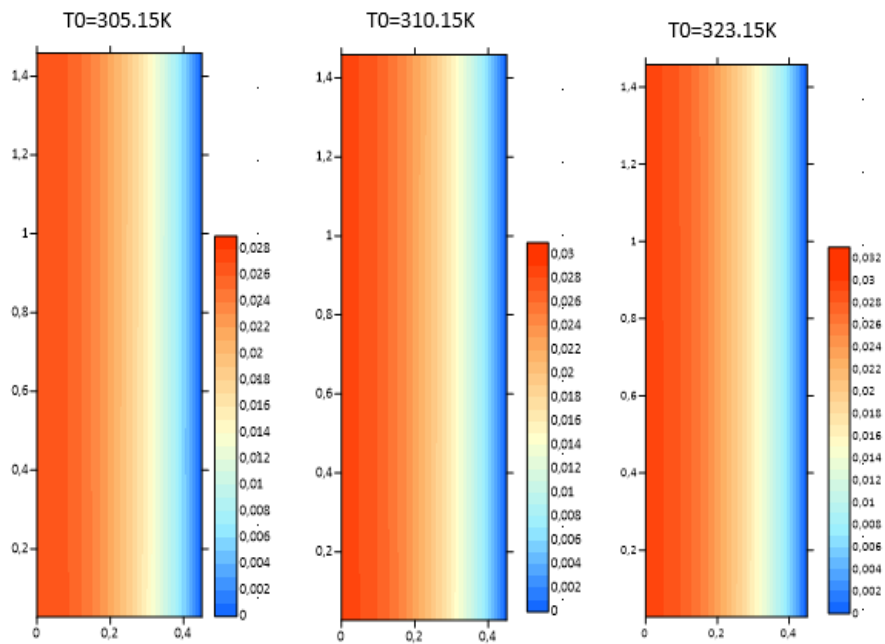
Figure 4. Velocity field as a function of fluid inlet temperature
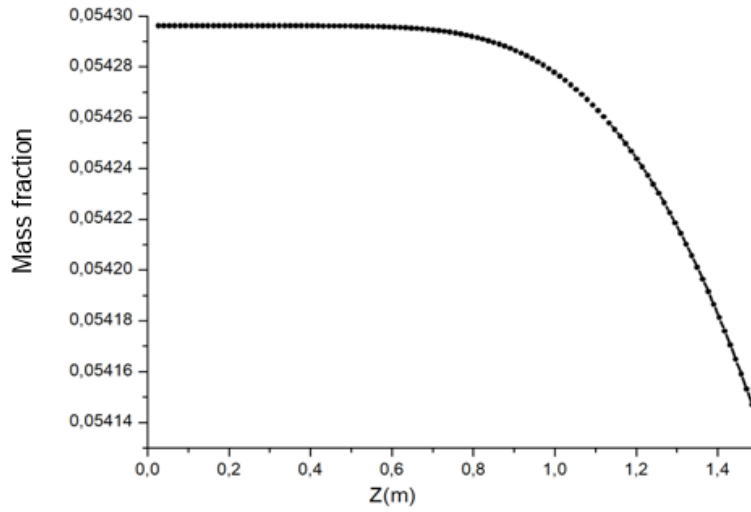
Figure 5. Axial evolution of mass fraction, for T0=323.15K and Re=500
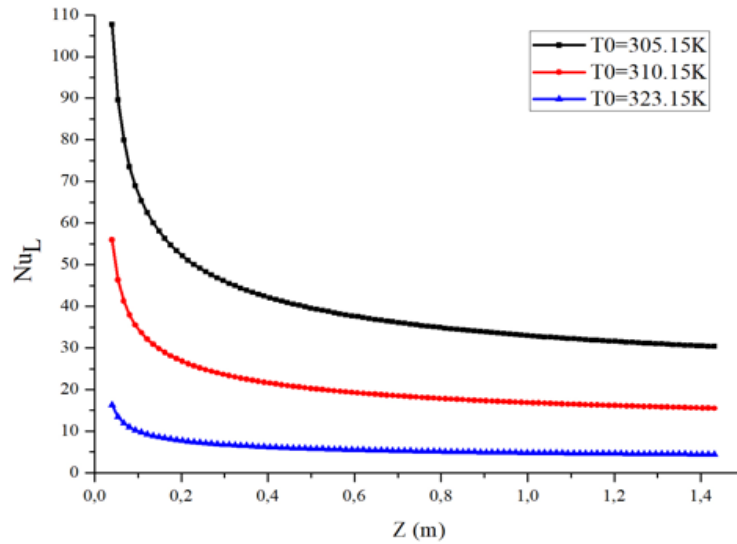
Figure 6. Evolution of latent Nusselt number as a function of fluid inlet temperature
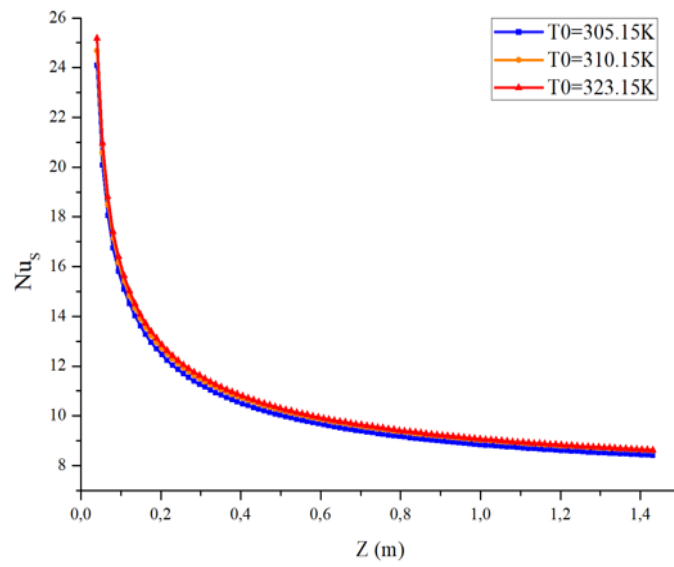
Figure 7. Evolution of Sensitive Nusselt number as a function of fluid inlet temperature
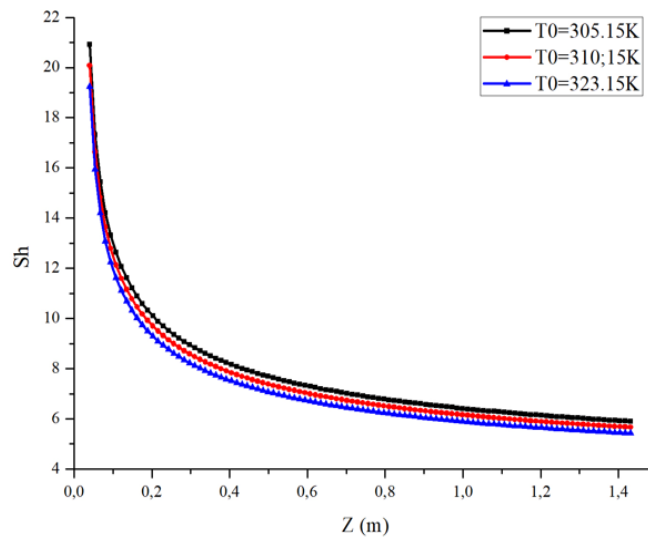
Figure 8. Evolution of Sherwood number as a function of fluid inlet temperature

Table 1. Dimensionless variables

Designation	Dimensionless variable
Radial coordinate	$x^\star = \dfrac{x}{Dh}$
Axial coordinate	$x^\star = \dfrac{x}{Dh}$
Radial velocity	$V^\star = \dfrac{V}{U_e}$
Temperature	$T^\star = \dfrac{T}{T_e}$
Pressure	$P^\star = \dfrac{P}{\rho_e U_e^2}$
Concentration	$C^\star = \dfrac{C}{C_e}$
Density	$\rho^\star = \dfrac{\rho}{\rho_e}$
Dynamic viscosity	$\vartheta^\star = \dfrac{\vartheta}{\vartheta_e}$
Thermal conductivity	$\lambda^\star = \dfrac{\lambda}{\lambda_e}$
Thermal diffusivity	$D^\star = \dfrac{D}{D_e}$
Specific heat	$Cp^\star = \dfrac{Cp}{Cp_e}$
Radius of channel	$R^\star = \dfrac{R}{Dh}$
Height of channel	$H^\star = \dfrac{H}{Dh}$
kinematic viscosity	$\boldsymbol{\mu^\star = \dfrac{\mu}{\mu_e}}$

Table 2. Grid independence

Grid(X*,Z*)	Z*=20	Z*=40	Z*=60	Z*=80
Values of $\mathrm{Nu_s}$				
(41x112)	8,0186	6,5718	5,9367	5,5652
(82x224)	8,7732	6,8555	5,9899	5,4705